Monthly Notices of the ROYAL ASTRONOMICAL SOCIETY

MNRAS **465,** 4434–4440 (2017) doi:10.1093/mnras/stw3047
Advance Access publication 2016 November 23

Thermal X-ray emission from massive, fast rotating, highly magnetized white dwarfs

D. L. Cáceres,[1,2] S. M. de Carvalho,[3] J. G. Coelho,[4] R. C. R. de Lima[2,5] and Jorge A. Rueda[1,2,6]★

[1]*Dipartimento di Fisica and ICRA, Sapienza Università di Roma, P.le Aldo Moro 5, I-00185 Rome, Italy*
[2]*ICRANet, P.zza della Repubblica 10, I-65122 Pescara, Italy*
[3]*Universidade Federal do Tocantins, Campus Araguaína, Av. Paraguai 77814-970 Araguaína, TO, Brazil*
[4]*Div. Astrofísica, Instituto Nacional de Pesquisas Espaciais, Av. dos Astronautas 1758, 12227–010 São José dos Campos, SP, Brazil*
[5]*Universidade do Estado de Santa Catarina, Av. Madre Benvenuta, 2007 Itacorubi, 88.035–901 Florianópolis, Brazil*
[6]*ICRANet-Rio, Centro Brasileiro de Pesquisas Físicas, Rua Dr. Xavier Sigaud 150, 2290–180 Rio de Janeiro, Brazil*

Accepted 2016 November 22. Received 2016 November 21; in original form 2016 February 5

ABSTRACT

There is solid observational evidence on the existence of massive, $M \sim 1\,M_\odot$, highly magnetized white dwarfs (WDs) with surface magnetic fields up to $B \sim 10^9$ G. We show that, if in addition to these features, the star is fast rotating, it can become a rotation-powered pulsar-like WD and emit detectable high-energy radiation. We infer the values of the structure parameters (mass, radius, moment of inertia), magnetic field, rotation period and spin-down rates of a WD pulsar death-line. We show that WDs above the death-line emit blackbody radiation in the soft X-ray band via the magnetic polar cap heating by back flowing pair-created particle bombardment and discuss as an example the X-ray emission of soft gamma-repeaters and anomalous X-ray pulsars within the WD model.

Key words: acceleration of particles – radiation mechanisms: thermal – stars: magnetic field – starspots – white dwarfs.

1 INTRODUCTION

The increasing data from observational campaigns leave no room for doubts on the existence of massive ($M \sim 1\,M_\odot$) white dwarfs (WDs) with magnetic fields comprised in the range $B = 10^6$–10^9 G (Külebi et al. 2009; Kepler et al. 2013, 2015). It has been recently shown that massive, highly magnetized WDs could be formed by mergers of double WDs (García-Berro et al. 2012). The fact that WDs produced in mergers, besides being massive and highly magnetized, can be also fast rotators with periods $P \sim 10$ s was used in Rueda et al. (2013) to show that they could be the WDs postulated in Malheiro, Rueda & Ruffini (2012) to describe the observational properties of soft gamma-repeaters (SGRs) and anomalous X-ray pulsars (AXPs), in alternative to the 'magnetar' model (Duncan & Thompson 1992; Thompson & Duncan 1995). In the WD model, the observed X-ray luminosity of SGRs/AXPs is explained via the loss of rotational energy of the fast rotating WD.[1] The WD gravitational stability imposes a lower bound to the rotation period $P \approx 0.5$ s, in agreement with the minimum measured rotation period of SGRs/AXPs, $P \sim 2$ s (Boshkayev et al. 2013b). On the other hand, the surface area and temperature of the emitting region inferred from the available infrared, optical and ultraviolet data of SGR/AXPs (i.e. for SGR 0418+5729, J1822.3–1606, 1E 2259+586 and 4U 0142+61) were shown to be consistent with the values expected from WDs (Boshkayev et al. 2013a; Rueda et al. 2013). The similarities of these WDs with ordinary, rotation-powered pulsars imply that similar radiation mechanisms are expected to be at work in their magnetosphere. Indeed, the loss of rotational energy of the WD, owing to magnetic breaking, is sufficient to explain the X-ray luminosity observed in SGRs/AXPs, and the inferred magnetic field from the observed spindown rates, $B \sim 10^9$ G, agrees with the aforementioned observed values in Galactic WDs (Malheiro et al. 2012; Coelho & Malheiro 2014).

Following this line, it was advanced in Rueda et al. (2013) that the blackbody observed in the soft X-rays of SGRs/AXPs, with observationally inferred radii $R_{\rm bb} \sim 1$ km and temperatures $T_{\rm bb} \sim 10^6$ K, could be due to a known phenomenon expected to occur in pulsars, namely the magnetospheric currents flowing back towards the WD, heating up the magnetic polar caps creating surface hot spots (see e.g. Usov 1988, 1993). The aim of this work is to estimate this

★ E-mail: jorge.rueda@icra.it

[1] It remains open the case of 1E 161348–5055, the central compact object in the supernova remnant RCW 103, to be confirmed as a new SGR/AXP (see e.g. Rea et al. 2016; D'Aì et al. 2016). The observed luminosity and light-curve periodicity with $P = 6.67$ h, if confirmed to be due to the rotation period, together with the upper limit of to the possible spin-down rate $|\dot{P}| < 7 \times 10^{-10}$, rule out the rotational energy of either a neutron star or a WD as the possible source of energy.

magnetospheric process for massive, highly magnetized, fast rotating WDs, exploiting the full analogy with pulsars. This calculation is interesting by its own and becomes of observational relevance in view of the latest results by Marsh et al. (2016) which point to the observational evidence of pulsar behaviour of a magnetized WD. It is interesting that, as in the well-known case of AE Aquari, also this WD belongs to a binary system. Pulsar behaviour can be observed from WDs in binaries when they can be considered approximately as isolated objects as in the case of detached binaries or in binaries in a propeller phase. White dwarf pulsars have been also considered as possible sources of high-energy and cosmic rays (see e.g. Kashiyama, Ioka & Kawanaka 2011). Bearing this in mind, we focus in this work on the observable emission from isolated magnetized WDs in the X-rays. In order to exemplify the mechanism with appealing numbers, we apply it to the case of the WD model of SGRs and AXPs. Specifically, we evaluate the decay rate of curvature radiation photons in e^-e^+ pairs, and the subsequent backward flow of pair-produced particles that bombards and heats up the magnetosphere polar caps, producing the observable thermal radiation. We compute in Section 2 the condition for e^-e^+ pair creation within the inner gap model. In Section 3, we calculate the expected thermal luminosity and infer the values of mass, radius, magnetic field and potential drop that ensure that the polar cap thermal emission explains the observed blackbody in the soft X-ray spectrum of SGRs/AXPs. The cases of 1E 2259+586 and 4U 0142+61 are analysed as specific examples. In Section 4, we simulate the observed X-ray flux from this spotty emission and compute the expected pulsed fraction, which we compare with the observed values in SGRs and AXPs. We outline the conclusions in Section 5.

2 WD MAGNETOSPHERE

Rotating, highly magnetized WDs can develop a magnetosphere analog to the one of pulsars. A corotating magnetosphere (Davis 1947; Ferraro & Unthank 1949; Gold 1962; Ferraro & Bhatia 1967) is enforced up to a maximum distance given by the so-called light cylinder, $R_{\rm lc} = c/\Omega = cP/(2\pi)$, where c is the speed of light and Ω is the angular velocity of the star, since corotation at larger distances would imply superluminal velocities for the magnetospheric particles. For an axisymmetric star with aligned magnetic moment and rotation axes, the local density of charged plasma within the corotating magnetosphere is (Goldreich & Julian 1969)

$$\rho_{\rm GJ} = -\frac{\boldsymbol{\Omega}\cdot\boldsymbol{B}}{2\pi c}\frac{1}{1-(\Omega r_\perp/c)^2}, \tag{1}$$

where $r_\perp = r\sin\theta$ with θ the polar angle.

The last B-field line closing within the corotating magnetosphere can be easily located from the B-field lines equation for a magnetic dipole $r/\sin^2\theta = \text{constant} = R_{\rm lc}$, and is located at an angle $\theta_{\rm pc} = \arcsin(\sqrt{R/R_{\rm lc}}) \approx \sqrt{R/R_{\rm lc}} = \sqrt{R\Omega/c} = \sqrt{2\pi R/(cP)}$ from the star's pole, with R the radius of the star. The B-field lines that originate in the region between $\theta = 0$ and $\theta = \theta_{\rm pc}$ (referred to as *magnetic polar caps*) cross the light cylinder, and are called 'open' field lines. The size of the cap is given by the polar cap radius $R_{\rm pc} = R\,\theta_{\rm pc} \approx R\sqrt{2\pi R/(cP)}$. Clearly, by symmetry, there are two (antipodal) polar caps on the stellar surface from which the charged particles leave the star moving along the open field lines and escaping from the magnetosphere passing through the light cylinder.

Particle acceleration is possible in regions called *vacuum gaps* where corotation cannot be enforced, i.e. where the density of charged particles is lower than the Goldreich–Julian value $\rho_{\rm GJ}$ given by equation (1). For aligned (anti-aligned) rotation and magnetic axes, we have $\rho_{\rm GJ} < 0$ ($\rho_{\rm GJ} > 0$), hence magnetosphere has to be supplied by electrons (ions) from the WD surface. This work is done by the existence of an electric field parallel to the magnetic field. Independently on whether $\boldsymbol{\Omega}\cdot\boldsymbol{B}$ is positive or negative, we assume that the condition of a particle injection density lower than $\rho_{\rm GJ}$ is fulfilled. In this *inner gap* model, the gaps are located just above the polar caps (Ruderman & Sutherland 1975) and the potential drop generated by the unipolar effect and that accelerates the electrons along the open B-field lines above the surface is

$$\Delta V = \frac{B_s \Omega h^2}{c}, \tag{2}$$

where h is the height of the vacuum gap and B_s is the surface magnetic field, which does not necessarily coincides with the dipole field B_p.

The electrons (or positrons) accelerated through this potential and following the B-field lines will emit curvature photons whose energy depends on the γ-factor, $\gamma = e\Delta V/(mc^2)$, where e and m are the electron charge and mass, and on the B-field line curvature radius r_c, i.e. $\omega_c = \gamma^3 c/r_c$. Following Chen & Ruderman (1993), we adopt the constraint on the potential ΔV for pair production via $\gamma + B \rightarrow e^- + e^+$,

$$\frac{1}{2}\left(\frac{e\Delta V}{mc^2}\right)^3 \frac{\lambda}{r_c}\frac{h}{r_c}\frac{B_s}{B_q} \approx \frac{1}{15}, \tag{3}$$

or in terms of a condition on the value of the potential,

$$\Delta V \approx \left(\frac{2}{15}\right)^{2/7}\left(\frac{r_c}{\lambda}\right)^{4/7}\left(\frac{\lambda\Omega}{c}\right)^{1/7}\left(\frac{B_s}{B_q}\right)^{-1/7}\frac{mc^2}{e}, \tag{4}$$

where we have used equation (2), $\lambda = \hbar/(mc)$, $B_q \equiv m^2c^3/(e\hbar) = 4.4\times10^{13}$ G, is the quantum electrodynamic field, with $\hbar$ the reduced Planck's constant.

For a magnetic dipole geometry, i.e. $B_s = B_d$ and $r_c = \sqrt{Rc/\Omega}$, the potential drop ΔV cannot exceed the maximum potential (i.e. for $h = h_{\rm max} = R_{\rm pc}/\sqrt{2}$),

$$\Delta V_{\rm max} = \frac{B_d \Omega^2 R^3}{2c^2}. \tag{5}$$

Here, we are interested in the possible magnetospheric mechanism of X-ray emission from magnetized WDs, thus we will consider the heating of the polar caps by the inward flux of pair-produced particles in the magnetosphere. These particles of opposite sign to the parallel electric field move inwards and deposit most of their kinetic energy on an area

$$A_{\rm spot} = f A_{\rm pc}, \tag{6}$$

i.e. a fraction $f \leq 1$ of the polar cap area, $A_{\rm pc} = \pi R_{\rm pc}^2$. The temperature $T_{\rm spot}$ of this surface hotspot can be estimated from the condition that it re-radiates efficiently the deposit kinetic energy, as follows. The rate of particles flowing to the polar cap is $\dot{N} = J A_{\rm pc}/e$, where $J = \eta\rho_{\rm GJ}c$ is the current density in the gap and $\eta < 1$ a parameter that accounts for the reduction of the particle density in the gap with respect to the Goldreich–Julian value (Cheng & Ruderman 1977 used $\eta = 1$ for order-of-magnitude estimates). In this model, the filling factor f is not theoretically constrained, and it has been estimated from pulsar's observations in X-rays that its value can be much smaller than unity (Cheng & Ruderman 1977). The condition that the hotspot luminosity equals the deposited kinetic energy rate reads

$$A_{\rm spot}\sigma T_{\rm spot}^4 = e\Delta V\dot{N} = J A_{\rm pc}\Delta V = \eta\rho_{\rm GJ}(R)cA_{\rm pc}\Delta V, \tag{7}$$

where σ is the Stefan–Boltzmann constant. From equations (1), (6) and (7), we obtain the spot temperature

$$T_{\rm spot} = \left(\eta \frac{B_d \Delta V}{\sigma f P}\right)^{1/4}. \quad (8)$$

It is worth mentioning that in the above estimate, we have assumed a full efficiency in the conversion from the deposited kinetic energy to the hotspot emission. This assumption is accurate if the heating source, namely the energy deposition, occurs not too deep under the star's surface and it is not conducted away to larger regions being mainly re-radiated from the surface area filled by the penetrating particles (Cheng & Ruderman 1980). In Appendix, we estimate the cooling and heating characteristic times and the heating and re-radiation efficiency. For the densities and temperatures of interest here, we show that the polar cap surface re-radiates efficiently most of the kinetic energy deposited by the particle influx validating our assumption.

3 SPECIFIC EXAMPLES

As in our previous analyses (Malheiro et al. 2012; Boshkayev et al. 2013a; Rueda et al. 2013; Coelho & Malheiro 2014), we use the traditional dipole formula to get an estimate for the WD dipole magnetic field, i.e.:

$$B_d = \left(\frac{3c^3}{8\pi^2}\frac{I}{R^6} P \dot{P}\right)^{1/2}, \quad (9)$$

where I is the moment of inertia of the star, $\dot{P} \equiv {\rm d}P/{\rm d}t$ is the first time derivative of the rotation period (spin-down rate) and an inclination of $\pi/2$ between the magnetic dipole and the rotation axis has been adopted. It is worth recalling that the estimate of the B-field by equation (9) is not necessarily in contrast, from the quantitative point of view, with an estimate using an aligned field but introducing a breaking from the particles escaping from the magnetosphere, since also in this case a quantitatively and qualitatively similar energy loss is obtained.

For a given rotation period P, the WD structure parameters such as mass M, radius R and moment of inertia I are bounded from below and above if the stability of the WD is requested (Boshkayev et al. 2013a). From those bounds, we established their lower and upper bounds for the field B_d of the WD.

3.1 1E 2259+586

We apply the above theoretical framework to a specific source, AXP 1E 2259+586. This source, with a rotation period $P = 6.98$ s (Fahlman & Gregory 1981) and a spin-down rate $\dot{P} = 4.8 \times 10^{-13}$ (Davies, Coe & Wood 1990), has a historical importance since Paczynski (1990) first pointed out the possibility of this object being a WD. This object produced a major outburst in 2002 (Kaspi et al. 2003; Woods et al. 2004), in which the pulsed and persistent fluxes rose suddenly by a factor of $\geq$20 and decayed on a time-scale of months. Coincident with the X-ray brightening, the pulsar suffered a large glitch of rotation frequency fractional change 4×10^{-6} (Kaspi et al. 2003; Woods et al. 2004). It is worth recalling that the observed temporal coincidence of glitch/bursting activity, as first pointed out by Usov (1994) in the case of 1E 2259+586, and then extended in Malheiro et al. (2012) and Boshkayev et al. (2013a), can be explained as due to the release of the rotational energy, gained in a starquake occurring in a total or partially crystallized WD. Since we are interested in the quiescent behaviour, we will not consider this interesting topic here. Therefore, only X-ray data prior to this outburst event will be used in this work (Zhu et al. 2008).

The soft X-ray spectrum of 1E 2259+586 is well fitted by a blackbody plus a power-law model. The blackbody is characterized by a temperature $kT_{\rm bb} \approx 0.37$ keV ($T_{\rm bb} \approx 4.3 \times 10^6$ K) and emitting surface are $A_{\rm bb} \approx 1.3 \times 10^{12}$ cm^2 (Zhu et al. 2008). These values of temperature and radius are inconsistent (too high and too small, respectively) with an explanation based on the cooling of a hot WD, and therefore such a soft X-ray emission must be explained from a spotty surface due to magnetospheric processes, as the one explored in this work.

The stability of the WD for such a rotation period constrains the WD radius to the range $R \approx (1.04–4.76) \times 10^8$ cm. For example, in the case of a WD with radius $R \approx 10^8$ cm, the polar cap area is $A_{\rm pc} = 6.6 \times 10^{14}$ cm, hence using equation (6) we have $f \approx 0.002$. From equation (8) the spot temperature $kT_{\rm spot} \approx 0.37$ keV can be obtained using $B_d \approx 6 \times 10^9$ G from the dipole formula (9), a potential drop $\Delta V \approx 3.5 \times 10^{11}$ V (lower than $\Delta V_{\rm max} \approx 5.4 \times 10^{12}$ V), and using the typical value $\eta = 1/2$ of the reduced particle density in the gap adopted in the literature. These parameters suggest a height of the gap, obtained with equation (2), $h \approx 0.11 R_{\rm pc}$.

The smallness of the filling factor, which appears to be not attributable to the value of h, could be explained by a multipolar magnetic field near the surface. It is interesting that the existence of complex multipolar magnetic field close to the WD surface is observationally supported (see e.g. Ferrario, de Martino & Gänsicke 2015). It is important to clarify that the above defined filling factor has only a physical meaning when, besides a strong non-dipolar surface field, the physical parameters of the star (magnetic field and rotational velocity) fulfill the requirement for the creation of electron–positron pairs in such a way that an avalanche of particles hits the surface. This is given by the request that the potential drop (4) does not exceed the maximum value (5). For example, for the largest magnetic field measured in WDs, $B \sim 10^9$G, and WD radii 10^8–10^9 cm, the maximum period that allows the avalanche of electron–positron pairs gives the range $P \sim$ 4–100 s, values much shorter than the value of typical rotation periods measured in most of magnetic WDs, $P \gtrsim 725$ s (see e.g. Ferrario et al. 2015). It is interesting to note that the condition of e^+e^- pair creation in the WD magnetosphere could explain the narrow range of observed rotation periods of SGRs/AXPs, $P \sim$ 2–12 s. Such a local, strong non-dipolar field in the surface diminishes the area bombarded by the incoming particles and, via magnetic flux conservation, the filling factor establishes the intensity of the multipolar magnetic field component as (see e.g. Cheng & Zhang 1999; Gil & Sendyk 2000; Gil & Melikidze 2002, and references therein)

$$B_s = \frac{B_d}{f}, \quad (10)$$

which implies that, close to the surface, there could be small magnetic domains with magnetic field intensity as large as 10^{11}–10^{12} G (see Fig. 1).

3.2 4U 0142+61

We can repeat the above analysis for the case of 4U 0142+61. This source, with a rotation period $P \approx 8.69$ s, was first detected by *Uhuru* (Forman et al. 1978). The measured period derivative of this source is $\dot{P} = 2.03 \times 10^{-12}$ (Hulleman, van Kerkwijk & Kulkarni 2000). The time-integrated X-ray spectrum of 4U 0142+61 is also described by a blackbody plus a power-law model. The blackbody component shows a temperature

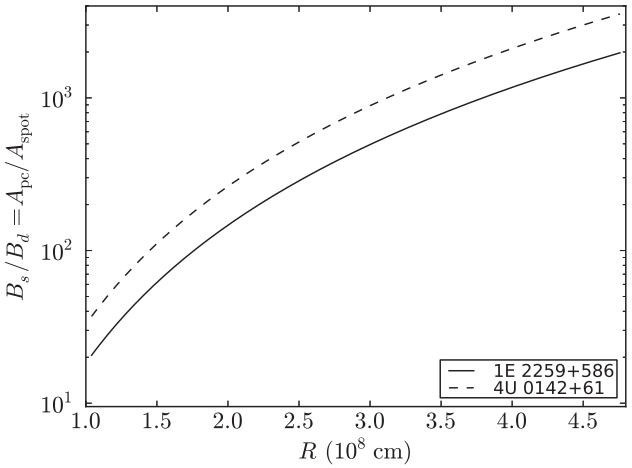

Figure 1. Surface to dipole magnetic field ratio given by magnetic flux conservation (10) for the AXPs 1E 2259+586 and 4U 0142+61.

$kT_{bb} = 0.39$ keV ($T_{bb} \approx 4.6 \times 10^6$ K) and a surface area $A_{bb} \approx 5.75 \times 10^{11}$ cm^2 (Göhler, Wilms & Staubert 2005). As for the above case of 1E 2259+5726, such a blackbody cannot be explained from the cooling of a WD but instead from a magnetospheric hotspot created by the heating of the polar cap.

For a WD radius $R = 10^8$ cm and a magnetic field $B_d \approx 10^{10}$ G for a rotating dipole (9), we have a filling factor $f \approx 0.001$, a potential drop $\Delta V \approx 1.4 \times 10^{11}$ V (smaller than $\Delta V_{max} \approx 5.8 \times 10^{12}$ Volts) and a gap height $h \approx 0.06 R_{pc}$. Again the filling factor suggests the presence of a strong multipolar component as shown in Fig. 1.

We show in Fig. 2 the potential drop inferred from equation (8) using the X-ray blackbody data for the above two sources. We check that for all the possible stable WD configurations, the potential drop satisfies the self-consistence condition $\Delta V < \Delta V_{max}$, where the latter is given by equation (5).

4 FLUX PROFILES AND PULSED FRACTION

We turn now to examine the properties of the flux emitted by such hot spots. Even if the gravitational field of a WD is not strong enough to cause appreciable general relativistic effects, for the sake of generality we compute the flux from the star taken into account

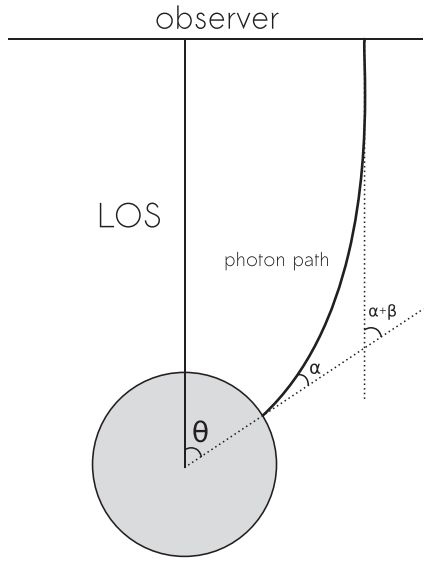

Figure 3. View of the photon trajectory and angles θ, α and β.

the bending of light. We shall follow here the treatment in Turolla & Nobili (2013) to calculate the observed flux that allows us to treat circular spots of arbitrary finite size and arbitrarily located in the star surface. The mass and radius of the star are denoted by M and R and the outer space–time is described by the Schwarzschild metric, i.e. we shall neglect at first approximation the effects of rotation. Let (r, θ, ϕ) be the spherical coordinate system centred on the star and the line-of-sight (LOS) the polar axis.

We consider an observer at $r \to \infty$ and a photon that arises from the star surface at $dS = R^2 \sin\theta d\theta d\phi$ making an angle α with the local surface normal, where $0 \leq \alpha \leq \pi/2$. The photon path is then bended by an additional angle β owing to the space–time curvature, reaching the observer with an angle $\psi = \alpha + \beta$. Since we have chosen the polar axis aligned with the LOS, it is easy to see that $\psi = \theta$ (see Fig. 3). Beloborodov (2002) showed that a simple approximate formula can be used to relate the emission angle α to the final angle θ:

$$1 - \cos\alpha = (1 - \cos\theta)\left(1 - \frac{R_s}{R}\right), \tag{11}$$

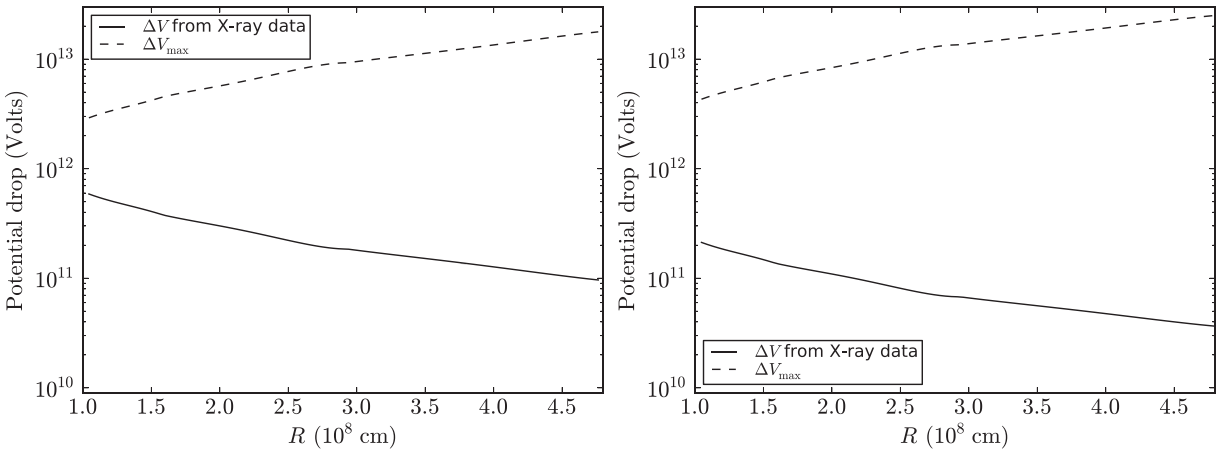

Figure 2. WD polar gap potential drop ΔV inferred via equation (8) using the blackbody observed in soft X-rays in 1E 2259+586 (left-hand panel) and 4U 0142+61 (right-hand panel). In this plot, we check the potential drop developed in the WD polar gap does not exceed the maximum potential reachable ΔV_{max} given by equation (5).

where $R_s = 2GM/c^2$ is the Schwarzschild radius and, as usual, G denotes the gravitational constant.

For an emission with a local Planck spectrum, the intensity is given by a blackbody of temperature T, $B_\nu(T)$, where ν is the photon frequency. The flux is proportional to the visible area of the emitting region (S_V) plus a relativistic correction proportional to the surface, given by the equation

$$F_\nu = \left(1 - \frac{Rs}{R}\right) B\nu(T) \int_{S_V} \cos\alpha \frac{\mathrm{d}cos\alpha}{\mathrm{d}(\cos\theta)} \mathrm{d}s$$
$$= \left(1 - \frac{Rs}{R}\right)^2 B_\nu(T)(I_p + I_s), \quad (12)$$

where

$$I_p = \int_{S_V} \cos\theta \sin\theta \mathrm{d}\theta\mathrm{d}\phi, \quad I_s = \int_{S_V} \sin\theta \mathrm{d}\theta\mathrm{d}\phi. \quad (13)$$

In polar coordinates, the circular spot has its centre at θ_0 and a semi-aperture θ_c. The spot is bounded by the function $\phi_b(\theta)$, where $0 \leq \phi_b \leq \pi$, and since we must consider just the star visible part, the spot must be also limited by a constant θ_F. For a given bending angle β, the maximum θ_F is given by the maximum emission α, i.e. $\alpha = \pi/2$. One can see that in a Newtonian gravity, where $\beta = 0$, the maximum visible angle is $\theta_F = \pi/2$, which means half of the star is visible, while in a relativistic star, values $\theta_F > \pi/2$ are possible, as expected. Then

$$I_p = 2\int_{\theta_{\min}}^{\theta_{\max}} \cos\theta \sin\theta\phi_b(\theta)\mathrm{d}\theta,$$
$$I_s = 2\int_{\theta_{\min}}^{\theta_{\max}} \sin\theta\phi_b(\theta)\mathrm{d}\theta, \quad (14)$$

where $\theta_{\min}$, $\theta_{\max}$ are the limiting values to be determined for the spot considered. Turolla & Nobili (2013) showed how to solve these integrals and how to treat carefully the limiting angles. The I_p and I_s integrals can be then written as $I_{p,s} = I_{1,2}(\theta_{\max}) - I_{1,2}(\theta_{\min})$ and we refer the reader to that work for the precise expressions.

Finally, the flux (12) is written as

$$F_\nu = \left(1 - \frac{Rs}{R}\right)^2 B_\nu(T) A_{\rm eff}(\theta_c, \theta_0), \quad (15)$$

where $A_{\rm eff}$ is the effective area, given by

$$A_{\rm eff}(\theta_c, \theta_0) = R^2 \left[\frac{Rs}{R} I_s + \left(1 - \frac{Rs}{R}\right) I_p\right]. \quad (16)$$

The total flux produced by two antipodal spots, with semi-apertures $\theta_{c,i}$ and temperatures T_i ($i = 1,2$), can be calculated by adding each contribution, so we have

$$F_\nu^{\rm TOT} = \left(1 - \frac{Rs}{R}\right)^2 [B_\nu(T_1) A_{\rm eff}(\theta_{c,1}, \theta_0)$$
$$+ B_\nu(T_2) A_{\rm eff}(\theta_{c,2}, \theta_0 + \pi/2)]. \quad (17)$$

Besides, the pulse profile in a given energy band $[\nu_1, \nu_2]$ for one spot is given by

$$F(\nu_1, \nu_2) = \left(1 - \frac{Rs}{R}\right)^2 A_{\rm eff}(\theta_c, \theta_0) \int_{\nu_1}^{\nu_2} B_\nu(T)\mathrm{d}\nu. \quad (18)$$

The star rotates with a period P (angular velocity $\Omega = 2\pi/P$), so we consider $\hat{\boldsymbol{r}}$ the unit vector parallel to the rotating axis. It is useful to introduce the angles ξ, the angle between the LOS (unit vector $\hat{\boldsymbol{l}}$) and the rotation axis and the angle χ between the spot axis (unit vector $\hat{\boldsymbol{c}}$) and the rotation axis, i.e. $\cos\xi = \hat{\boldsymbol{r}} \cdot \hat{\boldsymbol{l}}$ and $\cos\chi = \hat{\boldsymbol{r}} \cdot \hat{\boldsymbol{c}}$.

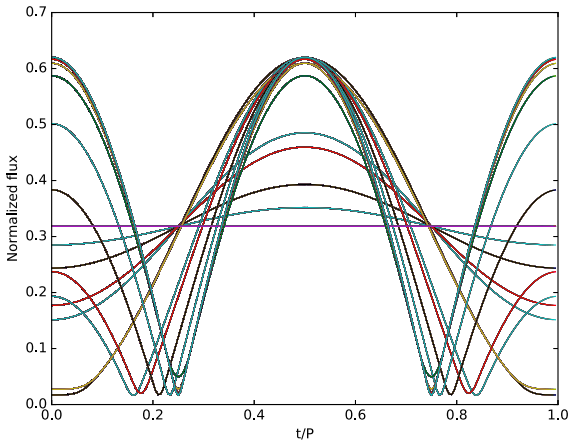

Figure 4. Flux profiles for different configurations of antipodal spots as a function of the phase. The semi-aperture for all the lines is $\theta_c = 3^\circ$. The WD parameters correspond to the ones of the WD of minimum radius adopted for AXP 1E 2259+586.

As the star rotates, the spot's centre, θ_0, changes. Let $\gamma(t) = \Omega t$ be the rotational phase, thus by geometrical reasoning we have

$$\cos\theta_0(t) = \cos\xi\cos\chi - \sin\xi\sin\chi\cos\gamma(t), \quad (19)$$

where it is indicated that ξ and χ do not change in time. When the total flux (17) is calculated for a given configuration (ξ, χ) in the whole period of time, the typical result is a pulsed flux with a maximum ($F_{\max}$) and a minimum flux ($F_{\min}$). As an example, we show in Fig. 4 flux profiles for different configurations of antipodal spots as a function of the phase for the WD of minimum radius in the case of AXP 1E 2259+586 used in Section 3.1.

We can measure the amount of pulsed emission by defining the *pulsed fraction*

$$\mathrm{PF} = \frac{F_{\max} - F_{\min}}{F_{\max} + F_{\min}}, \quad (20)$$

which we show in Fig. 5, as a function of the angles ξ and χ, for AXP 1E 2259+586. In the left-hand panel of this figure, we consider only the flux given by the blackbody produced by the two antipodal hotspots on the WD. We can see that indeed pulsed fractions as small as the above values can be obtained from magnetized WDs, for appropriate values of the geometric angles ξ and χ. However, the soft X-ray spectrum shows a non-thermal power-law component, additional to the blackbody one. As we have shown, the blackbody itself can contribute to the PF if produced by surface hotspots and thus the observed total PF of a source in those cases includes both contributions, mixed. It is thus of interest to explore this problem from the theoretical point of view. To do this, we first recall that total intrinsic flux of this source in the 2–10 keV band is $F_{\rm tot} \approx 1.4 \times 10^{-11}$ erg cm^{-2} s^{-1} and the power-law flux is $F_{\rm PL} \approx 1.8 F_{\rm bb} \approx 8.5 \times 10^{-12}$ erg cm^{-2} s^{-1} (Zhu et al. 2008). The right-hand panel of Fig. 5 shows the PF map for this source taking into account both the blackbody and the power-law components. By comparing this PF map with the one in the left-hand panel which considers only the pulsed blackbody we can see that they are very similar each other. This means that in these cases where both pulsed components are in phase and have comparable fluxes, it is difficult (although still possible if good data are available) to disentangle the single contributions.

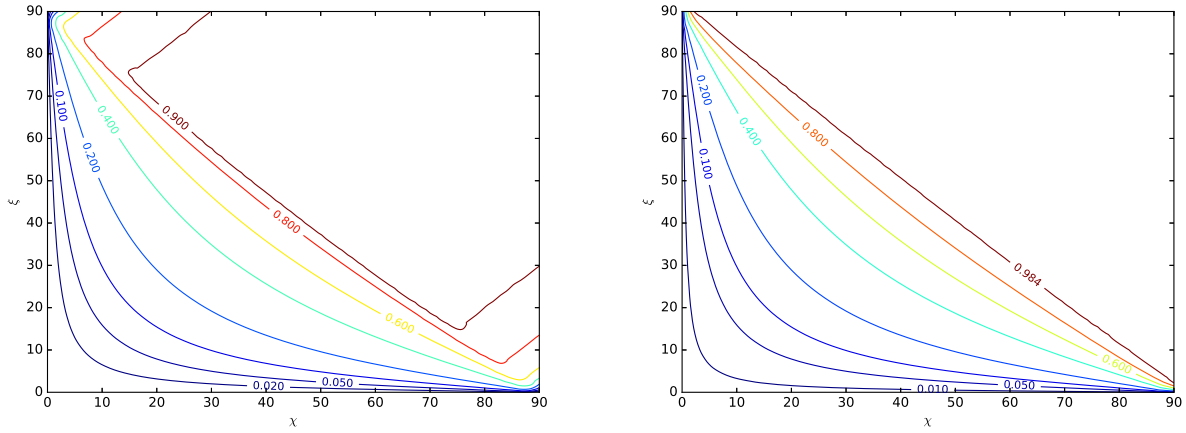

Figure 5. Theoretical PF as a function of the angles ξ and χ, computed in this work for the source 1E 2259+586 modelled as a WD of radius $R_{\rm min} \approx 1.04 \times 10^8$ cm. The left-hand panel shows the results of the PF produced by the blackbody given by the two antipodal hot spots. The right-hand panel shows the results for the total flux given by the blackbody plus the non-thermal power-law component, both pulsed. The observed total PF of this source in the 2–10 keV is about 20 per cent (Zhu et al. 2008).

5 CONCLUSIONS

We exploited the analogy with pulsars to investigate whether or not massive, highly magnetized, fast rotating WDs can behave as neutron star pulsars and emit observable high-energy radiation. We conclude the following:

(i) We showed that WDs can produce e^-e^+ pairs in their magnetosphere from the decay of curvature radiation photons, i.e. we infer the structure parameters for which they are located above the WD pulsar death-line. We evaluated the rate of such a process. Then, we calculated the thermal emission produced by the polar cap heating by the pair-created particles that flow back to the WD surface due to the action of the induction electric field.

(ii) In order to give a precise example of the process, we applied the theoretical results to the case of the WD model of SGRs and AXPs. We have shown that the inferred values of the WD parameters obtained from fitting with this magnetospheric emission, the blackbody spectrum observed in the soft X-rays of SGRs and AXPs, are in agreement with our previous estimates using the IR, optical, and UV data and fall within the constraints imposed by the gravitational stability of the WD.

(iii) We have related the size of the spot with the size of the surface under the polar cap filled by the inward particle bombardment. We have shown that the spot area is much smaller than the polar cap area pointing to the existence of strong non-dipolar magnetic fields close to the WD surface.

(iv) We have used the heat transport and energy balance equations to show that for the actual conditions of density and temperature under the polar cap, the hotspot re-radiates efficiently the heat proportioned by the inward particle bombardment.

(v) The spot, which is aligned with the magnetic dipole moment of the WD, produces a pulsed emission in phase with the rotation period of the object. We showed that the theoretically inferred pulsed fraction of the WD spans from very low values all the way to unity depending on the viewing angles. Therefore, it can also account for the observed pulsed fraction in SGRs and AXPs for appropriate choices of the viewing angles. In addition, the low-energy tail of the blackbody spectrum of the hotspot could produce a non-null pulsed fraction of the flux in the optical bands as well. However, this depends on the flux produced by the surface temperature of the WD which certainly dominates the light curve at low energies. From the quantitative point of view, the size of the surface area of the spots is crucial for the explanation of the observed pulsed fraction in soft X-rays.

(vi) We have also shown that the addition of a pulsed power-law component as the one observed in SGRs/AXPs does not modify appreciably the above result. The reason for this is that the non-thermal power-law component and the blackbody due to the surface hotspot have comparable fluxes and are in phase with each other. In those cases, it is difficult to disentangle the siingle contributions to the pulsed fraction.

We have shown that, as advanced in Rueda et al. (2013), indeed the blackbody observed in the optical wavelengths of SGRs and AXPs can be due to the surface temperature of the WD, while the one observed in the X-rays can be of magnetospheric origin. For the power-law component, also observed in the soft X-rays, a deeper analysis of processes, such as curvature radiation, inverse Compton scattering, as well as other emission mechanisms, is currently under study.

There is also room for application and extension of the results presented in this work to other astrophysical phenomena. WD mergers can lead to a system formed by a central massive, highly magnetized, fast rotating WD, surrounded by a Keplerian disc (see Rueda et al. 2013, and references therein). At the early stages, the WD and the disc are hot and there is ongoing accretion of the disc material on to the WD. In such a case, the WD surface shows hot regions that deviate from the spotty case, e.g. hot surface rings. That case is also of interest and will be presented elsewhere.

ACKNOWLEDGEMENTS

It is a great pleasure to thank M. Malheiro for thoughtful discussions and for the comments and suggestions on the presentation of our results. Likewise, we would like to thank N. Rea. We are grateful to L. Becerra for providing us tables of the heat capacity and thermal conductivity in the range of densities and temperatures of interest for this work. DLC acknowledges the financial support by the International Relativistic Astrophysics (IRAP) Ph. D. Program. JGC, RCRL, SMC and JAR acknowledge the support by the International Cooperation Program CAPES-ICRANet financed by CAPES – Brazilian Federal Agency for Support and

Evaluation of Graduate Education within the Ministry of Education of Brazil. JGC acknowledges the support of FAPESP through the project 2013/15088–0 and 2013/26258–4.

REFERENCES

Beloborodov A. M., 2002, ApJ, 566, L85
Boshkayev K., Izzo L., Rueda Hernandez J. A., Ruffini R., 2013a, A&A, 555, A151
Boshkayev K., Rueda J. A., Ruffini R., Siutsou I., 2013b, ApJ, 762, 117
Chabrier G., Potekhin A. Y., 1998, Phys. Rev. E, 58, 4941
Chen K., Ruderman M., 1993, ApJ, 402, 264
Cheng A. F., Ruderman M. A., 1977, ApJ, 214, 598
Cheng A. F., Ruderman M. A., 1980, ApJ, 235, 576
Cheng K. S., Zhang L., 1999, ApJ, 515, 337
Coelho J. G., Malheiro M., 2014, PASJ, 66, 14
D'Aì A. et al., 2016, MNRAS, 463, 2394
Davies S. R., Coe M. J., Wood K. S., 1990, MNRAS, 245, 268
Davis L., 1947, Phys. Rev., 72, 632
Duncan R. C., Thompson C., 1992, ApJ, 392, L9
Fahlman G. G., Gregory P. C., 1981, Nature, 293, 202
Ferrario L., de Martino D., Gänsicke B. T., 2015, Space Sci. Rev., 191, 111
Ferraro V. C. A., Bhatia V. B., 1967, ApJ, 147, 220
Ferraro V. C. A., Unthank H. W., 1949, MNRAS, 109, 462
Forman W., Jones C., Cominsky L., Julien P., Murray S., Peters G., Tananbaum H., Giacconi R., 1978, ApJS, 38, 357
García-Berro E. et al., 2012, ApJ, 749, 25
Gil J., Melikidze G. I., 2002, ApJ, 577, 909
Gil J. A., Sendyk M., 2000, ApJ, 541, 351
Gil J., Melikidze G. I., Geppert U., 2003, A&A, 407, 315
Göhler E., Wilms J., Staubert R., 2005, A&A, 433, 1079
Gold T., 1962, J. Phys. Soc. Japan Suppl., 17, A187
Goldreich P., Julian W. H., 1969, ApJ, 157, 869
Hulleman F., van Kerkwijk M. H., Kulkarni S. R., 2000, Nature, 408, 689
Itoh N., Hayashi H., Kohyama Y., 1993, ApJ, 418, 405
Kashiyama K., Ioka K., Kawanaka N., 2011, Phys. Rev. D, 83, 023002
Kaspi V. M., Gavriil F. P., Woods P. M., Jensen J. B., Roberts M. S. E., Chakrabarty D., 2003, ApJ, 588, L93
Kepler S. O. et al., 2013, MNRAS, 429, 2934
Kepler S. O. et al., 2015, MNRAS, 446, 4078
Külebi B., Jordan S., Euchner F., Gänsicke B. T., Hirsch H., 2009, A&A, 506, 1341
Malheiro M., Rueda J. A., Ruffini R., 2012, PASJ, 64, 56
Marsh T. R. et al., 2016, Nature, 537, 374
Paczynski B., 1990, ApJ, 365, L9
Potekhin A. Y., Chabrier G., 2000, Phys. Rev. E, 62, 8554
Rea N., Borghese A., Esposito P., Coti Zelati F., Bachetti M., Israel G. L., De Luca A., 2016, ApJ, 828, L13
Ruderman M. A., Sutherland P. G., 1975, ApJ, 196, 51
Rueda J. A., Boshkayev K., Izzo L., Ruffini R., Lorén-Aguilar P., Külebi B., Aznar-Siguán G., García-Berro E., 2013, ApJ, 772, L24
Thompson C., Duncan R. C., 1995, MNRAS, 275, 255
Tsai Y.-S., 1974, Rev. Mod. Phys., 46, 815
Turolla R., Nobili L., 2013, ApJ, 768, 147
Usov V. V., 1988, Sov. Astron. Lett., 14, 258
Usov V. V., 1993, ApJ, 410, 761
Usov V. V., 1994, ApJ, 427, 984
Woods P. M. et al., 2004, ApJ, 605, 378
Zhu W., Kaspi V. M., Dib R., Woods P. M., Gavriil F. P., Archibald A. M., 2008, ApJ, 686, 520

APPENDIX: HEATING AND COOLING OF PARTICLE INFLUX BOMBARDMENT

We estimate in this appendix the efficiency of the particle bombardment in heating (and re-rediating) the surface area they hit. We follow the discussion in Gil & Melikidze (2002), Gil, Melikidze & Geppert (2003) for the heat flow conditions in the polar cap surface of neutron stars, and extended it to the present case of magnetized WDs.

The particles arriving to the surface penetrate up to a depth that can be estimated using the concept of *radiation length* (Cheng & Ruderman 1980). For a carbon composition, the radiation length is $\Sigma \approx 43\ \mathrm{g\ cm^{-2}}$ (Tsai 1974), so an electron would penetrate the WD surface up to a depth

$$\Delta z \approx \frac{\Sigma}{\rho} = 4.3 \times 10^{-3}\ \mathrm{cm} \left(\frac{10^4\ \mathrm{g\ cm^{-3}}}{\rho} \right). \tag{A1}$$

With the knowledge of the thickness of the layer under the surface where the energy deposition occurs, we can proceed to estimate the properties of the diffusion and re-radiation of the kinetic energy of the particle influx using the heat transport and energy balance equations on the star's surface corresponding to the polar cap. The typically small distances (see equation A1) allow us to introduce a plane-parallel approximation in the direction parallel to the magnetic field lines, say in the direction z orthogonal to the surface.

The energy balance can be simply written as

$$F_{\mathrm{rad}} = F_{\mathrm{heat}} + F_{\mathrm{cond}}, \tag{A2}$$

where $F_{\mathrm{heat}} = e\Delta V \eta \rho_{\mathrm{GJ}} c$, $F_{\mathrm{cond}} = -\kappa\, \partial T/\partial z$ and $F_{\mathrm{rad}} = \sigma T^4$, with κ the thermal conductivity (along the z-direction).

Let us first estimate the characteristic cooling time. To do this, we switch off energy losses and heating terms in the energy balance equation (A2), i.e. the radiation flux is only given by conduction:

$$\sigma T^4 = -\kappa \frac{\partial T}{\partial z}, \tag{A3}$$

which leads to the heat transport equation

$$c_v \frac{\partial T}{\partial t} = \frac{\partial}{\partial z} \left(\kappa \frac{\partial T}{\partial z} \right), \tag{A4}$$

where c_v is the heat capacity per unit volume. We can therefore obtain the characteristic (e-folding) cooling and heating time assuming the quantities are uniform within the penetration depth Δz, i.e.

$$\Delta t_{\mathrm{cool}} = \frac{\Delta z^2 c_v}{\kappa}, \qquad \Delta t_{\mathrm{heat}} = \frac{c_v \Delta z}{\sigma T^3}. \tag{A5}$$

We can now introduce the radiation to heating efficiency parameter

$$\epsilon \equiv \frac{F_{\mathrm{rad}}}{F_{\mathrm{heat}}} = \frac{1}{1 + \Delta t_{\mathrm{heat}}/\Delta t_{\mathrm{cool}}} = \frac{1}{1 + \kappa/(\sigma T^3 \Delta z)}, \tag{A6}$$

which shows that in equilibrium, $\Delta t_{\mathrm{heat}} = \Delta t_{\mathrm{cool}}$, we have $\epsilon = 1/2$.

In estimating the spot temperature (8), we have assumed in equation (7) full re-radiation of the influx, namely we assumed $\epsilon = 1$. We proceed now to estimate the realistic values of ϵ from equation (A6) to check our assumption. We compute the thermal conductivity from Itoh, Hayashi & Kohyama (1993) and the heat capacity from Chabrier & Potekhin (1998); Potekhin & Chabrier (2000). For example, at a density $\rho = 10^3\ \mathrm{g\ cm^{-3}}$ and $T = 10^6$ K, we have $c_v = 2.7 \times 10^{10}\ \mathrm{erg\ cm^{-3}\ K^{-1}}$ and $\kappa \approx 4 \times 10^{11}\ \mathrm{erg\ cm^{-1}\ s^{-1}\ K^{-1}}$, and equation (A6) gives $\epsilon \approx 0.86$. At $T = 10^7$ K, we have $c_v = 3.8 \times 10^{11}\ \mathrm{erg\ cm^{-3}\ K^{-1}}$ and $\kappa \approx 3.4 \times 10^{13}\ \mathrm{erg\ cm^{-1}\ s^{-1}\ K^{-1}}$ and $\epsilon \approx 1$.

This paper has been typeset from a TEX/LATEX file prepared by the author.